


RESEARCH ARTICLE

WILEY

Geomorphological and meteorological drivers of ephemeral pond hydrology in the Canadian shield forest

Marjolaine Roux¹ | Marie Larocque¹  | Philippe Nolet² |
 Mohammad Bizhanimanzar^{1,3}

¹Geotop Research Center, GRIL Research Center and Département des Sciences de la Terre et de l'atmosphère, Université du Québec à Montréal, Montréal, Canada

²Département des Sciences Naturelles and Institut des Sciences de la Forêt Tempérée (ISFORT), Université du Québec en Outaouais (UQO), Ripon, Canada

³Climate Change, Resilience and Sustainability, WSP Canada, Montréal, Canada

Correspondence

Marie Larocque, Geotop Research Center, GRIL Research Center and Département des Sciences de la Terre et de l'atmosphère, Université du Québec à Montréal, Montréal, Québec, Canada.
 Email: larocque.marie@uqam.ca

Funding information

Natural Sciences and Engineering Research Council of Canada

Abstract

Ephemeral ponds in cold and humid forested regions are often vulnerable because of their small size and ephemeral nature. The aim of this study was to identify the geomorphological and meteorological drivers of ephemeral pond hydrology in the forests of cold and humid climates. A multi-year study of 40 ponds was conducted in the Kenauk forest located in the Canadian Shield of the Outaouais region (Quebec, Canada). Pond bathymetry, mineral and organic sediment thickness, watershed area, slope, canopy cover and maximum depth were measured in-situ. The spring hydroperiod (the period during which there is water in the ponds between April and October) as well as the surface and groundwater recession rates were measured throughout the study period, from 2016 to 2020. Data from this study show that ponds located at lower altitudes in the landscape are larger, receive water from a larger area, and have longer hydroperiods than ponds located at higher altitudes. The results demonstrated a connection between the ponds and the surrounding aquifer. Spring and early summer precipitation was shown to affect hydroperiods the most, while summer precipitation influenced the presence of water in the ponds from April to October. Winter precipitation appear determinant for pond recession rates. Simple multiple regression models were able to simulate hydroperiods and hydroperiod indices relatively well, but pond recession rates were not well represented by the models. This study brings original multi-year and multi-site data identifying parameters and variables that determine ephemeral pond hydrology in cold and humid climates. The results provide new insights into their resilience on the landscape and bring new arguments for their long-term protection.

KEYWORDS

Canadian Shield, ephemeral ponds, forest, geomorphology, hydrology, meteorological variables

1 | INTRODUCTION

Ephemeral ponds can be found in the northeast region of North America and are also called temporary ponds or vernal ponds. These ponds are small wetlands consisting of depressions of various shapes, depths,

and positions across the landscape (Brooks & Hayashi, 2002; Tiner, 2003). The seasonal wetlands in this region are active in the spring following snowmelt and dry in early summer. The scientific literature recognizes that although they appear to be isolated from nearby hydrosystems, ephemeral ponds are connected through runoff and

This is an open access article under the terms of the [Creative Commons Attribution-NonCommercial-NoDerivs](https://creativecommons.org/licenses/by-nc-nd/4.0/) License, which permits use and distribution in any medium, provided the original work is properly cited, the use is non-commercial and no modifications or adaptations are made.

© 2023 The Authors. *Hydrological Processes* published by John Wiley & Sons Ltd.

groundwater flow exchanges (Bertassello et al., 2018; Hayashi et al., 2016; Malzone et al., 2019; Pyzoha et al., 2008). Ephemeral ponds are strong contributors to forest diversity. The ephemeral nature of these ponds makes them particularly attractive breeding habitats for woodland amphibians and invertebrates that can thrive there due to the absence of fish (Calhoun et al., 2003; Colburn, 2004; Werner et al., 2007). Although they are omnipresent in humid forests of cold and humid climates, ephemeral ponds are vulnerable due to their size, and apparent limited connectivity to forest hydrology. Because they can be overlooked during the dry season, they are often not included in wetlands maps. These ponds are therefore susceptible to disappearing, either naturally or due to human interventions, and their disappearance may go unnoticed (Hunter et al., 2017).

The last two decades has seen an increase in the scientific literature on ephemeral ponds. Local studies on ephemeral pond hydrology have focused on the period following freshet during which the ponds hold water, known as the hydroperiod. Studies have reported how the ephemeral pond hydroperiod is influenced by meteorological conditions such as precipitation and evapotranspiration, as well as geographical and geological conditions such as vegetation cover, basin morphometry, topography, and geology (Bauder, 2005; Bertassello et al., 2022; Brooks, 2004; Malzone et al., 2019; Skidds & Golet, 2005). Local in-situ studies are often based on a small number of ephemeral ponds, but some authors have conducted multi-site studies (e.g., Bertassello et al., 2022; Skidds & Golet, 2005). Recent studies have also focused on understanding their hydrology at the local scale, for example, by using relatively simple water budget calculations (e.g., Bertassello et al., 2018; Pyke, 2005). Others have used approaches such as machine-learning models and other modelling techniques to predict ephemeral pond inundation (Cartwright et al., 2021), water storage volume (Cui et al., 2021), and contribution to wetland discharge (Klammler et al., 2020).

Many questions remain about ephemeral pond hydrology, especially their connectivity to groundwater and the size of their contributing areas. Multi-year field data are needed to monitor both surface water conditions (in the ponds) and groundwater conditions (in the saturated geological media). This type of study has been conducted in South Carolina, United States (e.g., Pyzoha et al., 2008) as well as in the Prairie pothole region (e.g., Hayashi et al., 2016), but there are few such studies. Recent studies have focused on the hydrological functions of geographically isolated wetlands at the landscape scale (e.g., Cohen et al., 2016; Evenson et al., 2018; McLaughlin et al., 2014; Neff et al., 2020; Rains et al., 2016), including water storage in surface depressions and water transmission to overflows and underlying aquifers. However, a better understanding of all the components of pond hydrology is necessary to assess more fully their hydrological functions. Although some authors argue that prolonged multi-year hydrologic monitoring might not be necessary to understand the suitability of the ponds as breeding habitats (e.g., Skidds & Golet, 2005), many questions remain as to how geomorphologic and meteorologic conditions influence their hydrological variables. A growing number of studies are investigating the way in which anthropogenic pressures and climate change are expected to impact ephemeral ponds (e.g., Cui et al., 2021; Pyke, 2005). However, further

investigation is needed to determine whether the drivers of pond hydrology contribute to pond hydrological resilience in a changing climate.

The aim of this study was to identify the geomorphological and meteorological drivers of ephemeral pond hydrology in the forested areas of northeast North America. To achieve this objective, 40 ephemeral ponds located in a forest in the Canadian Shield, in the Outaouais region (Quebec, Canada), were studied over a five-year period. This study provides a unique and original database on ephemeral pond hydrology. It also provides insights for future research to improve the understanding of wetland dynamics at the landscape scale, including for example a better identification and protection of potential amphibian habitats and a better understanding of the variability and vulnerability of ephemeral pond hydrology.

2 | STUDY AREA

The study area is the Kenauk Nature private forest (257 km²) in the Outaouais region of southern Quebec, Canada (Figure 1) in the Grenville geological province. The Canadian Shield bedrock is composed of intrusive, magmatic, and metasedimentary Precambrian rocks (Hynes et al., 2010) and is marked by many shallow depressions from past glaciations. The area is covered with layers of discontinuous and continuous Quaternary till and fluvio-glacial and glaciomarine sediments (Daigneault et al., 2012) in the lower elevations of the Kinonge River valley. Bedrock outcrops cover 6% of the territory.

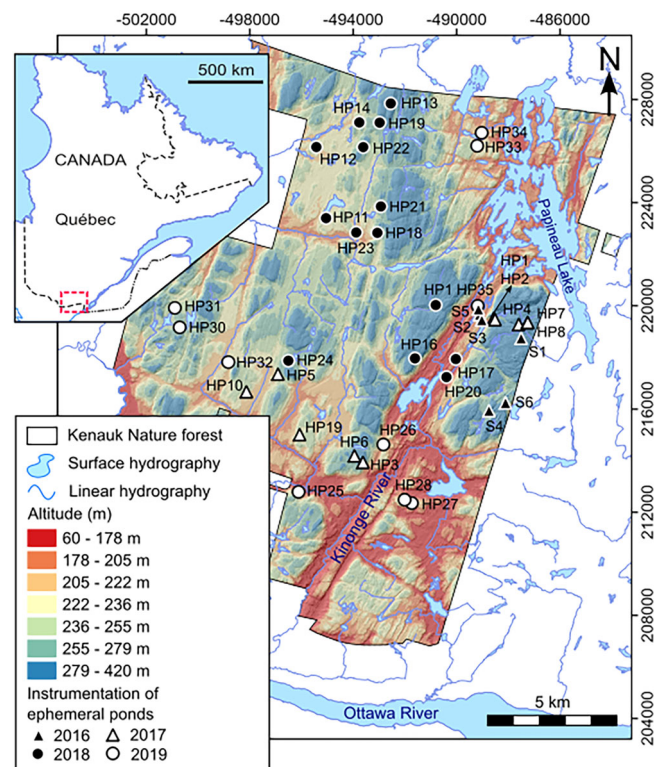


FIGURE 1 Location of the study area within the Kenauk Nature forest (Outaouais region, Québec and Canada) and instrumented ephemeral ponds.

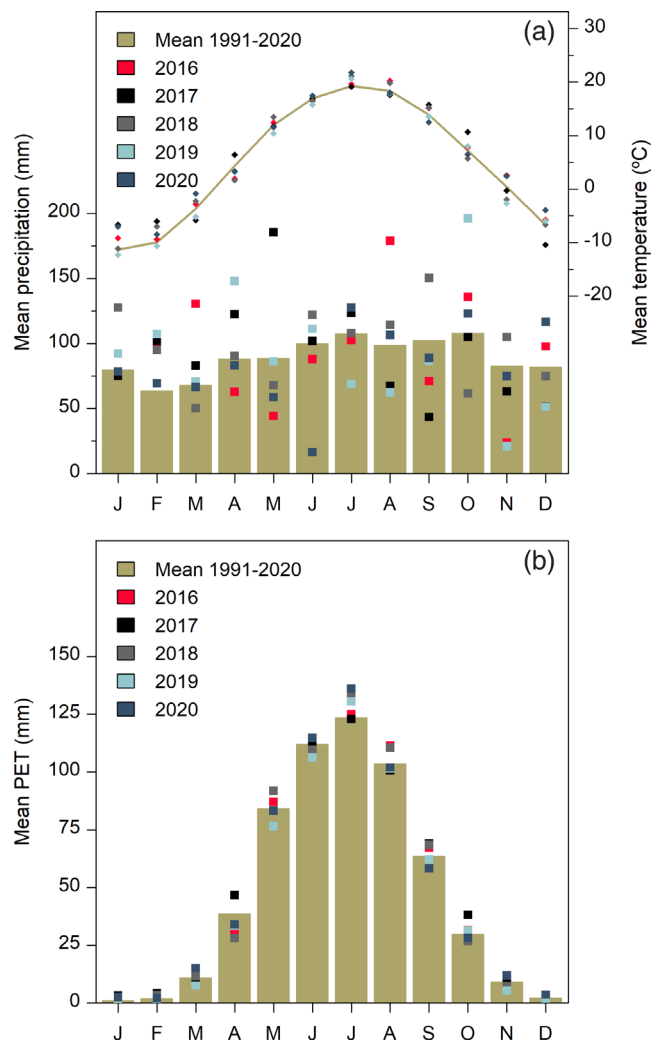


FIGURE 2 Meteorological data for long-term conditions (1991–2020) and for 2016–2020 showing (a) precipitation and temperature and (b) potential evapotranspiration.

Elevations across the study area range from 65 to 420 m. Rivers and lakes cover 10% of the study area, forests cover 77% (47% hardwood species, 22% mixed species, 8% of softwood species; Forget et al., 2006; Varin et al., 2015), and wetlands cover 13%. Wetland types are primarily peatlands, but swamps are also abundant (DUC, 2017). Bournival et al. (2017) estimated that ephemeral ponds represent 0.7% of the area.

Precipitation and temperature data up to 2016 are available from the Climate Quebec gridded dataset (Bergeron, 2016). An on-site meteorological station located near the Papineau Lake outlet has been providing daily precipitation and temperature data since 2016 (Figure 2). The 1991–2020 average annual precipitation (P) is 1090 mm, with 24% of the total precipitation falling as snow between November and April. For the same period, the interannual average temperature was 5.1°C, and the annual potential evapotranspiration (PET) calculated with daily temperatures using the Oudin et al. (2005) formula was 579 mm.

The five-year study period had relatively stable annual precipitation, ranging between 964 mm (2020) and 1061 mm (2017). However, monthly precipitation markedly varied between 2016 and 2020, with very dry months (minimum of 17 mm in June 2020) and wet months (maximum of 196 mm in October 2020). Average annual temperatures ranged between 4.2°C (2019) and 6.1°C (2016 and 2017). Mean monthly temperatures revealed that the coldest month was January 2019 (−12.3°C) and the warmest was July 2020 (21.8°C). Potential evapotranspiration (PET) varied annually between 556 (2019) and 607 (2018) mm/yr, with a maximum monthly PET in July 2020 (136 mm). The complete monthly and annual values for P, temperature, and PET are listed in Table S1 (Supplementary Material).

3 | METHODS

3.1 | Ephemeral pond selection

Forty ephemeral ponds were monitored and characterized in this study (Figure 1; Table S2, Supplementary Material). Six ponds were selected and instrumented in spring 2016, 10 more were added in 2017, 14 were added in 2018 and 10 were added in 2019. Monitoring stopped in July 2020. The ponds were selected based on five criteria defined by Bournival et al. (2017). To be selected, the ponds must (1) be isolated from any other surface water body (by >10 m), (2) have an area < 5000 m², (3) have water depths between 0.1 and 2 m, (4) contain no vegetation as this can indicate permanent inundation, and (5) have a mineral substrate that is covered by at least a minimal layer of organic matter. Two ponds (HP7 and HP8) were located very close together (<10 m apart), thus forming a pond complex.

3.2 | Instrumentation and monitoring

Water levels were measured in all the ponds using piezometers, which are 2.54 cm diameter PVC tubes with perforations in the lower 20 cm (Figure 3). The piezometers that were installed on top of the organic litter in the deepest area of each pond were called SW piezometers. The piezometers were instrumented with Solinst level loggers that monitored hourly water levels. For ponds S1–S6, similar tubes were used to install piezometers in the mineral deposits using a manual auger. Below the ponds (GWB piezometers), depths ranged between 93 and 270 cm from the bottom of the pond, and outside the pond (GWO piezometers), depths ranged from 55 to 176 cm from the surface. These piezometers were also instrumented with Solinst level loggers that monitored hourly groundwater levels. Data from a local Solinst barometer were used to compensate for atmospheric pressure for all water levels. Water level monitoring was interrupted between November 2016 and April 2017, but in ponds where water levels exceeded 0.2 m in late fall, loggers were not removed during the winters that followed.

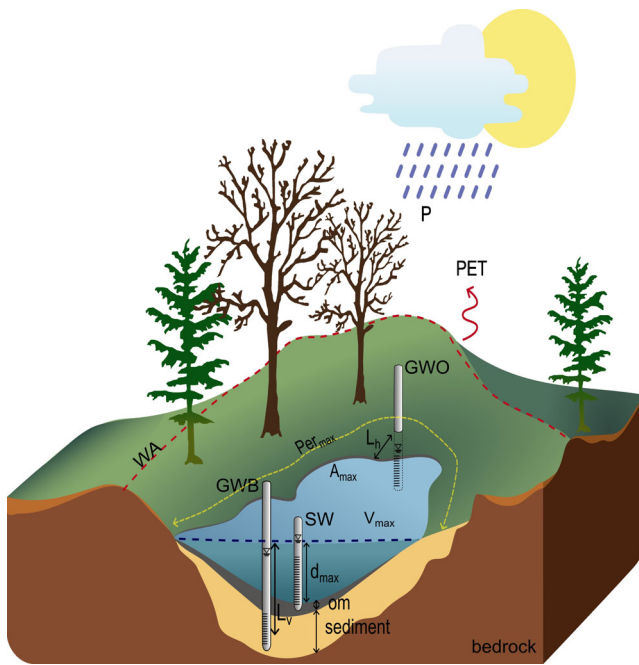


FIGURE 3 Typical instrumentation of ephemeral ponds. Note that only ponds S1–S6 are instrumented with GWB and GWO piezometers.

3.3 | Pond morphometry and geomorphological setting

Sediment thickness was measured during the dry season (June to August) using a 4 cm manual auger along a transect that followed the longest axis of the ponds. The measured thickness of the mineral sediments and the organic matter represent the difference between the topography and the bedrock, except at sites HP17, HP20, and HP31, where the bedrock was too deep to be reached. At each site, four surveys were conducted outside the ponds and seven to 11 surveys were conducted below the ponds. Sediment types were determined visually in-situ.

Pond bathymetry, necessary to determine pond volume and area, was measured with a Leica TC805L total station. Many bathymetric survey points were measured along transects that were perpendicular to the longest pond axis, with distances between transects ranging between 1.5 m (S1–S6 and HP1–HP10) and 6 m (HP11–HP35). The bathymetric survey could not be completed at HP13 because of the presence of vegetation inside the pond. The relative elevations were associated with the regional topography using LiDAR data with 1 m horizontal resolution (absolute horizontal and vertical accuracy of 30 cm; Varin et al., 2021).

Pond areas and volumes were calculated in ArcGIS at 0.1 m water depth intervals using bathymetry data. Together with the monitored water levels, these data provided the necessary information to estimate pond depths, maximum surface areas, and volumes. Brooks and Hayashi (2002) suggested using these values in Equation (1) to derive a basin profile parameter p that represents pond geometry for ponds in bedrock depressions similar to those in this study. Equation (1) was

used with the field-measured values of V_{max} , A_{max} and d_{max} to derive p values for each pond:

$$V_{max} = \frac{A_{max} \times d_{max}}{1 + \frac{2}{p}}, \quad (1)$$

where V_{max} is the maximum pond volume (m^3), A_{max} is the maximum pond area (m^2), d_{max} is the maximum water depth in the pond (m), and p is the shape parameter ($p < 1$ is convex, $p > 1$ is concave, and $p = 1$ is a straight slope).

Watershed areas (WA) that contribute to the pond were calculated using the Hydrology Tools in the ArcGIS 10.5 software package with the LiDAR data. Pond altitude and the average slope of the pond watershed were also derived from the LiDAR data.

The percentage of canopy cover was measured between June and August, in 2016 or 2019, using a spherical densiometer. For each pond, five locations were selected for collecting measurements, one at the pond centre and four near the edge of the pond. A reading was taken in all four cardinal directions at each location (Palik et al., 2007). The canopy cover was calculated from the average readings from all locations.

3.4 | Hydrological variables

The spring hydroperiod (SHP) refers to the period starting at the spring freshet during which the ponds hold water and which ends in late spring or early summer. In this study, the end of the SHP was the first day of the year when the water level in the pond fell below 0.02 m. To estimate the fraction of the year during which the ponds were active, the hydroperiod index (HPI) was calculated as the number of days during which the pond contained standing water divided by the number of days between April 1st and October 15th. This period was selected as it included the monitored months for all the ponds between 2016 and 2019 (2020 is excluded from HPI calculations because monitoring stopped in July). An HPI equal to one represents a pond that never dried during this period, while an HPI of 0 represents a pond that did not hold any water that year.

The recession rate (RR) is the midnight-to-midnight water level change, calculated following the method from Chandler et al. (2017). Surface water RR values were calculated using all available data between April 1st and October 15th. Groundwater recession rates were calculated only after the pond became dry and include recessions that lasted longer than 48 hours after a water level increase. Normalized recession rates (NRR) were calculated following Malzone et al. (2019) as the ratio between RR and potential evapotranspiration (PET). The PET was calculated using the formula from Oudin et al. (2005) based on daily temperature data. The normalization was applied to surface water levels (NRR_{sw} , SW piezometers) and groundwater levels (NRR_{gw} , GWB piezometers in ponds S1 to S6), with the hypothesis that evapotranspiration can affect both reservoirs. Values of $NRR_{sw} > 1$ indicate pond recession rates larger than PET, meaning

the pond emptied more rapidly than it would have if evapotranspiration were the only pond outflow:

$$NRR_{sw} = \frac{RR_{sw}}{PET}. \quad (2)$$

$$NRR_{gw} = \frac{RR_{gw}}{PET}. \quad (3)$$

Daily vertical (i_v) and horizontal (i_h) hydraulic gradients between the aquifer and the pond were calculated for ponds S1 to S6 to provide an estimate of groundwater–surface water flow exchange. The vertical hydraulic gradients (i_v) were calculated by dividing the difference between the average daily head in the GWB piezometer (h_{GWB}) and the average daily water level in the SW piezometer (h_{SW}) by the vertical distance between the surface water level and the mid-screen elevation of the GWB piezometer (L_v). The horizontal hydraulic gradients (i_h) were calculated by dividing the difference between the average daily head in the GWO piezometer (h_{GWO}) and the average daily water level in the SW piezometer by the horizontal distance between the two measurements (L_h). Positive hydraulic gradients indicate potential groundwater flow from the aquifer to the pond.

$$i_v = \frac{h_{GWB} - h_{SW}}{L_v}. \quad (4)$$

$$i_h = \frac{h_{GWO} - h_{SW}}{L_h}. \quad (5)$$

3.5 | Correlation and multiple linear regression

The Multi Linear Regression (MLR) model provides several benefits for the analysis of multidimensional systems where the response variable is regulated by the interaction of a variety of unrelated factors, such as physical characteristics of the pond, as well as meteorological conditions. The MLR model can also reveal the relative ability of each explanatory variable to explain the variations of the response variable.

To construct the MLR model for *SHP* prediction, the following conditions were met: (1) a linear relationship existed between the explanatory variables and the hydrological variables (preliminary tests were performed, but are not shown here; other model forms were tested but showed no clear evidence of superiority); (2) there was no multicollinearity, meaning the physical and meteorological variables were not correlated with each other; (3) the observations were independent of each other; (4) the homoscedasticity hypothesis applied, meaning the variance of the residuals did not follow a specific pattern; and (5) the multivariate normality hypothesis applied, meaning MLR residuals followed a normal distribution. The MLR analyses were performed using the Python *statmodels* software package (R Core Team, 2020).

The approach used was explicitly modulated to identify the simplest MLR models to verify causal relationships between explanatory variables and hydrological variables. A Student's *t*-test (*stats* package in R; R Core Team, 2020) was used to differentiate annual averages

for *SHP* and *HPI* and site averages for i_v and i_h . Correlations between morphometry and geomorphological parameters (the correlations referred to herein as *physical parameters*) were quantified using a Spearman rank correlation coefficient (r_s), which was also used to assess the correlation between physical parameters and hydrological variables (*SHP*, *HPI*, NRR_{sw} , NRR_{gw} , i_h and i_v). A similar procedure was applied to assess the correlation between precipitation (P) and net precipitation (Pnet = P–PET) and hydrological variables. Correlations with individual months and with groups of successive months for P and Pnet were tested. Note that the correlation between Pnet and NRR_{sw} and NRR_{gw} was not assessed, as PET is used in Equation (2). Statistical tests were conducted using the *Hmisc* (Spearman correlation) and *stats* (Student's *t*-test) packages (R Core Team, 2020). A multiple linear regression (MLR) model was thus developed using a combination of the meteorological variable and of the physical parameter that separately have the highest correlations (r_s) with the modelled hydrological variable:

$$hydro_{var} = \alpha(met_{var}) + \beta(phys_{par}) + \varepsilon, \quad (6)$$

where $hydro_{var}$ represents one hydrological variable, met_{var} represents the meteorological variable, and $phys_{par}$ represents the physical parameter. Terms α and β are the coefficients of the multiple regression, and ε represents the variations of $hydro_{var}$ that are not represented by either met_{var} or $phys_{par}$.

4 | RESULTS

4.1 | Pond morphometry and geomorphological settings

The ponds were located at altitudes ranging between 168 m (HP20) and 366 m (HP7). They were found in bedrock depressions that were elongated along one axis. Except for ponds S3, HP35, and HP6, all the sites had an outlet where overflow occurred when the ponds were filled. The bedrock depressions were covered by a layer of organic matter and mineral sediments of variable thicknesses (Table S2, Supplementary Material). The thickness of organic matter at the bottom of the ponds varied from 12 cm (HP6) to 124 cm (HP17), with the maximum thickness typically occurring in the center of the pond and gradually thinning towards the edges. Mineral sediments included clay (at sites located below 212 m in ponds S2, S5, HP17, HP20, HP25, and HP26), silt, and fine, medium, and coarse sand. Mineral sediments were absent below the organic matter at site HP27.

The maximum pond area (A_{max}) ranged from 23.4 m² (HP7) to 1808.8 m² (HP26), while the maximum pond volume (V_{max}) varied between 1.3 m³ (HP4) and 710.4 m³ (S3). The maximum water levels (d_{max}) were generally observed between April and June, ranging from 0.12 m (HP27) to 2.09 m (S3). The maximum pond perimeter (Per_{max}) varied between 25.1 m (HP7) and 414.6 m (HP26) (Table S2, Supplementary Material). The basin profile coefficient p varied between 0.54 (HP2, convex slope) and 4.70 (HP27, concave slope).

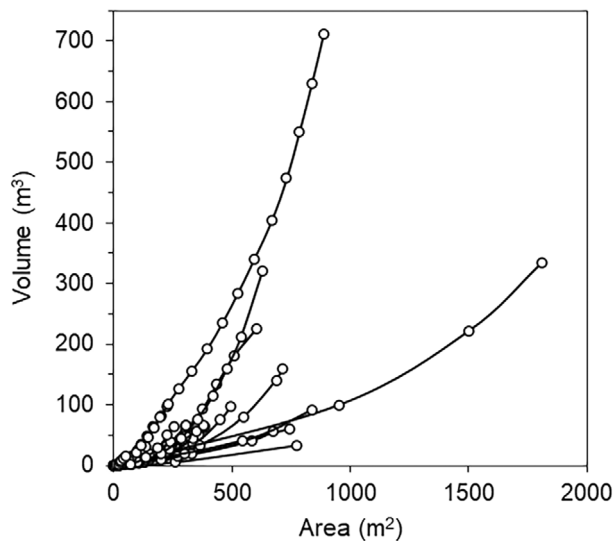


FIGURE 4 Volume-area relationship for all the ponds.

The volume-area relationships of the ponds (Figure 4) showed remarkable differences between ponds with low volumes and large surface areas (e.g., HP26) and those with high volumes and small surface areas (e.g., S3). Pond watershed areas (WAs) ranged between 373 m² (S4) and 17 973 m² (HP24). The average slopes of the watersheds ranged from 4.4° (HP24) to 20.3° (HP4). The ratios between the watershed area and the maximum pond area (WA/A_{max}) ranged from 3.6 (HP27) to 170.7 (HP4).

In general, trees were located outside the ponds and around pond margins where water depths remained shallow. Canopy cover varied between 40% (HP14) and 92% (HP9).

4.2 | Pond hydrology

The SW piezometers revealed that all the ponds had similar hydrological patterns throughout the year. The ponds partially filled in September and October due to more frequent rainfall events and lower evapotranspiration (Figure 5 for ponds S1 to S6, and Figure S1

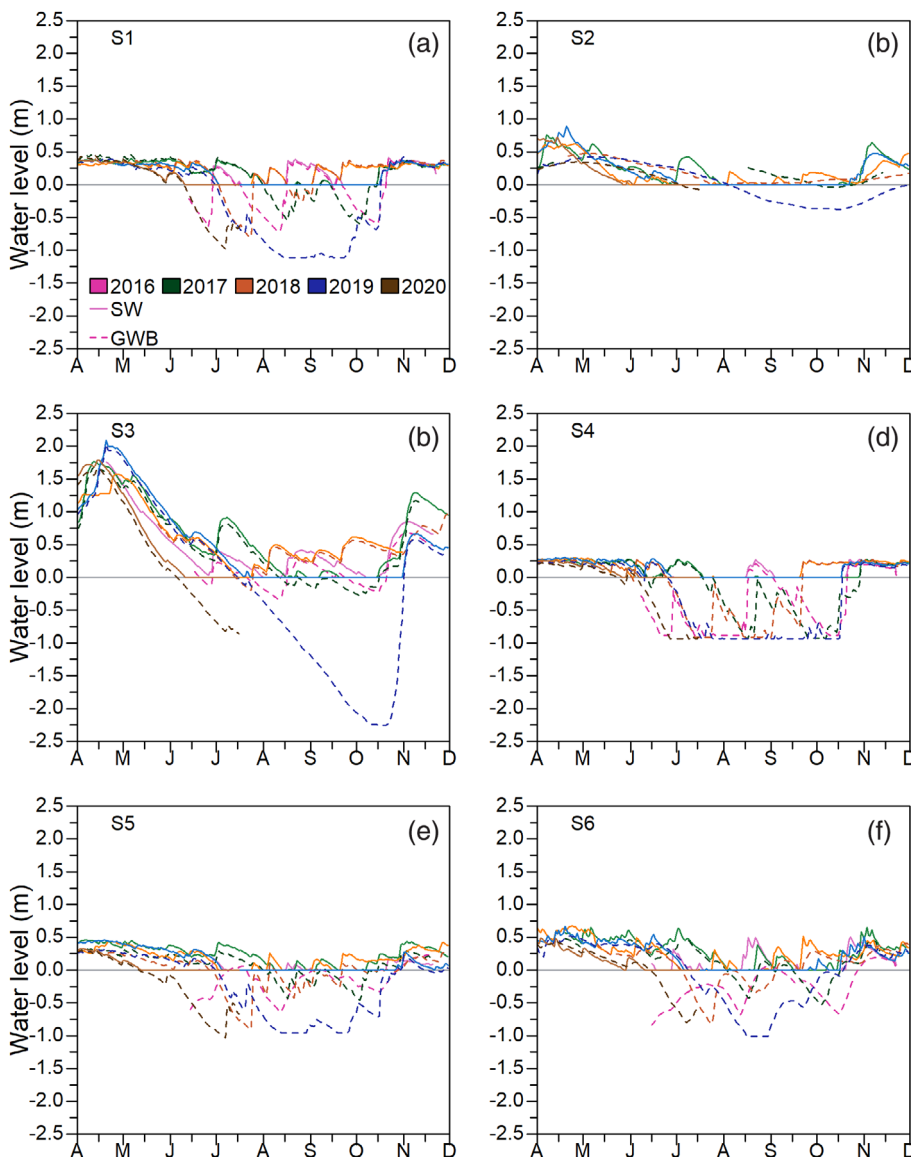


FIGURE 5 Surface water levels (SW piezometers) and groundwater levels below the ponds (GWB piezometers) for ponds S1–S6. The horizontal grey line represents the pond bottom.

Supplementary Material). The ponds probably remained active throughout the winter but because of the ice and snow cover, winter water levels (when available) were excluded from the analysis. The ponds generally reached their maximum water levels (d_{max}) at the onset of spring rain and snowmelt, which occurred on April 15th (2016), March 29th (2017), April 14th (2018), April 06th (2019), and March 27th (2020). Subsequently, the ponds gradually emptied through the months of May and June and were generally dry by the end of June. The ponds temporarily refilled during summer after significant rainfall events but then rapidly emptied again. All ponds became dry during the summer, even in the wettest year in 2017. During a particularly dry summer in 2019, the ponds did not refill for approximately 3 months. Conversely, during a wet summer in 2016, the ponds frequently became temporary refilled. Interestingly, ponds S1 to S6 also had marked differences in surface and groundwater level fluctuations (Figure 5). For example, S3 which is the largest pond with a GWB piezometer, had the more variable surface water levels while the smallest pond S4 had the least variable surface water levels. Site S2, one of the two ponds where clay was observed in the sediments, had the shallowest groundwater levels.

Because three (S2, S3, and S6) out of six ponds were already dry when monitoring started in May and early June 2016, *SHP* values for that year were only available for three ponds. *SHP* was also not calculated for HP2 in 2017 due to technical difficulties (see Table S2 Supplementary Material). The median values for *SHP*s were 63 days (2016), 85 days (2017), 80 days (2018), 89 days (2019) and 60 days (2020) for all sites, with a minimum *SHP* of 22 days (HP9 in 2020) and a maximum *SHP* of 139 days (S3 in 2017) (Figure 6a). Average *SHP*s varied significantly from year to year, but they were significantly lower in 2020 compared to 2017, 2018 and 2019 (Student's *t*-test, $p < 0.05$).

The *HPI* medians were 0.80 (2016), 0.68 (2017), 0.77 (2018), and 0.48 (2019) (Figure 6b; Table S2, Supplementary Material), with a minimum of 0.39 (HP6 in 2019) and a maximum of 0.96 (S3 in 2018) (Figure 5 and Figure S1). Average *HPI* values did not vary significantly from year to year, except in 2019, which had a significantly lower *HPI* compared to previous years (Student's *t*-test, $p < 0.05$).

4.3 | Pond-groundwater connectivity

GWB piezometers for ponds S1–S6 (Figure 5) showed that groundwater levels were highest between April and the end of June, and between mid-October and the end of December. Groundwater level variations were similar for all the years and for all the ponds, except S2. At site S2, the GWB piezometer intercepted low-permeability clay sediments, which seems to have induced a delayed signal after precipitation and snowmelt. During a dry period in July and August 2019, the water table dropped below the loggers at sites S1, S3, S4, S5, and S6, leading to the temporary interruption of groundwater level monitoring.

The median values of the normalized recession rates for the pond water levels (NRR_{sw}) varied between 2.6 (HP17) and 12.4 (HP6)

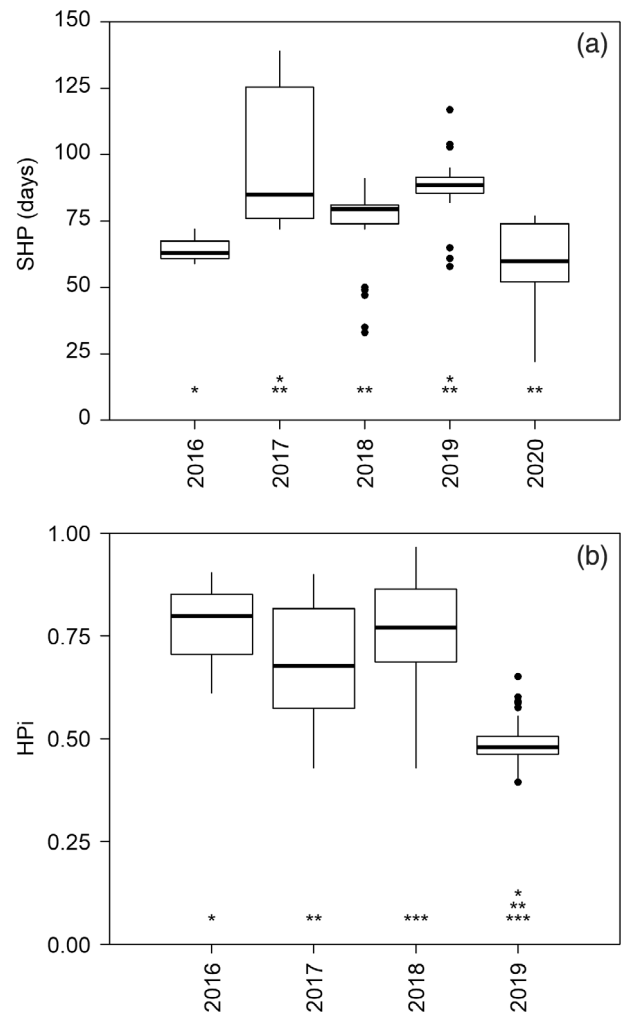


FIGURE 6 Boxplots of (a) spring hydroperiods (*SHP*) and (b) hydroperiod indices (*HPI*) of the studied ponds between 2016 and 2020. Three ponds were monitored in 2016, 15 in 2017, 30 in 2018, 40 in 2019 and 14 in 2020. Years with the same symbol (*, **, ***) have averages that are significantly different (Student's *t*-test, $p < 0.05$).

(Table S3 Supplementary Material). HP17 had the least varied NRR_{sw} values, while values for HP23 were the most varied (Figure 7). NRR_{sw} values were >1 for all the ponds.

The median horizontal hydraulic gradients (i_h) between 2016 and 2020 varied between 0.01 (S6), indicating lateral inflow from the sediments to the pond, and -0.03 (S4), indicating lateral outflow from the pond to the sediments (Figure 8). Pond S4 had the largest range for i_h while pond S3 has the smallest range. The average i_h values over the study period for sites S1 to S6 were significantly different between sites (Student's *t*-test, $p < 0.05$), except for sites S3 and S6.

The median vertical hydraulic gradients (i_v) between 2016 and 2020 varied between 0.10 (S6), indicating upward flow from the sediments to the pond, and -0.23 (S5), indicating downward flow from the pond to the sediments (Figure 8). Pond S2 had the largest range for i_v values between the 25% and 75%, likely due to the position of the piezometer in the clay sediments. Pond S6 stood out with positive

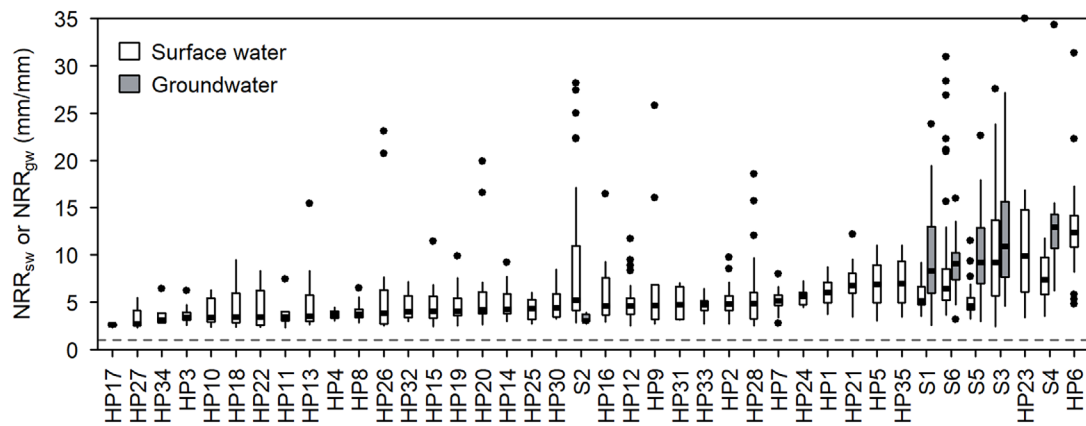


FIGURE 7 Boxplots of normalized recession rates for surface water levels (NRR_{sw} for SW piezometers) and groundwater levels (NRR_{gw} for GWB piezometers) at all the ponds. The dashed horizontal line represents $NRR_{sw} = 1$ for which the pond recession rate equals PET.

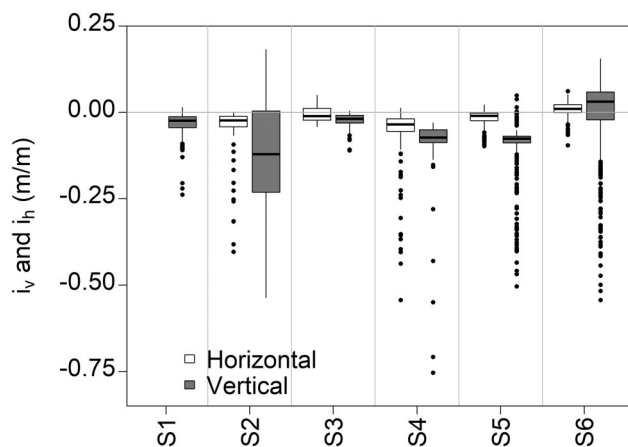


FIGURE 8 Boxplots of horizontal hydraulic gradients (i_h) between SW and GWO piezometers and of vertical hydraulic gradients (i_v) between SW and GWB piezometers at ponds S1–S6. The horizontal grey line represents i_h or $i_v = 0$.

median i_h and i_v values, indicating dominating lateral inflow and vertical inflow. The average i_v values over the study period for sites S1–S6 were significantly different between sites (Student's t -test, $p < 0.05$), except between sites S1 and S3 and sites S4 and S5.

4.4 | Explanatory factors

Correlations between physical parameters (altitude, organic matter thickness, sediment thickness, A_{max} , V_{max} , Per_{max} , p , WA, slope, WA/A_{max} , canopy cover, and d_{max}) showed that many of the physical parameters were significantly correlated (Figure S2). The ponds located at the lowest altitude had the maximum sediment thickness, the largest A_{max} , V_{max} , Per_{max} , WA, and an average watershed slope. The organic matter layer was thickest in ponds with the smallest d_{max} . The ponds with large A_{max} , V_{max} , Per_{max} values were those with the thickest sediments. The largest ponds (high A_{max}) had higher V_{max} ,

Per_{max} , Per_{max}/A_{max} , p , and WA values as well as smaller WA/A_{max} and smaller canopy cover. The ponds with the largest volumes (high V_{max}) also had the longest Per_{max} and the highest d_{max} , as well as the lowest WA/A_{max} , canopy cover and d_{max} . The basin profile parameter p was largest when WA/A_{max} was small. Unsurprisingly, WA was positively correlated with WA/A_{max} , but also inversely correlated with canopy cover.

Correlations between physical parameters and hydrological variables SHP , HPi , NRR_{sw} , NRR_{gw} , i_h and i_v for all the years revealed that many variables are significantly correlated (Figure S3). SHP and HPi were sometimes positively correlated with sediment thickness, A_{max} , V_{max} , Per_{max} , and WA, and negatively correlated with canopy cover. NRR_{sw} was largest for ponds with small areas (low A_{max}) and short perimeters (low Per_{max}) in 2018 and 2019. It was also largest for ponds with the smallest contributing area (WA), but only in 2018. NRR_{sw} was positively correlated with canopy cover in 2018 and with d_{max} in 2017 and 2019. NRR_{gw} had few correlations with physical parameters. The high correlations observed in 2016 could be due to the limited number of monitored ponds that year. From 2017 to 2020, NRR_{gw} did not show any statistically significant correlations with the physical parameters. Both i_h and i_v showed few significant correlations with the physical parameters. However, in 2017 and 2018, i_h was positively correlated with WA/A_{max} and in 2018, i_v was negatively correlated with p .

Correlations between meteorological variables and the six hydrological variables for all years revealed many statistically significant results for SHP , HPi and NRR_{sw} (Figure S4). NRR_{gw} , i_h , and i_v showed almost no correlations with meteorological variables and were not pursued further. Higher P or Pnet values yielded longer $SHPs$, with similar significant correlations for different groups of successive months, but the highest correlation was found for spring months (i.e., from February–April to May–June, $r_s = 0.61$ or 0.62). The results show that smaller HPi values resulted from more P or Pnet for the groups of successive months starting in early spring to mid-summer (i.e., April–May, April–June, April–July, and May–June, $r_s = -0.34$).

For the other groups of months that started later and extended later into the summer, higher P or Pnet led to higher *HPI* values. This indicates that the precipitation in spring and summer influences *HPI* differently. The results also show that NRR_{sw} decreased when P increased, with the highest correlations for groups of successive winter months (i.e., January–April and February–April, $r_s = -0.39$).

Per_{max} was selected as the $phys_{par}$ because it had the highest correlation with *SHP*, *HPI*, and NRR_{sw} . Because the results showed that Pnet did not improve the simulation of *SHP* or *HPI* and because it was not tested for NRR_{sw} , P was used as the met_{var} . Groups of successive months with the highest r_s values were tested in the MLR analysis. The March–June period resulted in the highest r_s values for the *SHP* MLR model, while June–August was the best period for the *HPI* MLR model. The January–April period resulted in the highest r_s values for the NRR_{sw} MLR model. The best NRR_{sw} model was found when using the logarithm of NRR_{sw} . The results from the null hypothesis $Pr(>|t|)$ for all three MLR models and their ability to predict the hydrological variables of the ponds were examined. Combinations of the maximum pond perimeter and precipitation for a given period were found to perform significantly better than the simple regression model based on physical parameters or meteorological variables individually (Table 1). The standardized regression coefficients showed that in the three MLR models, met_{var} had a greater effect on MLR (more than two times in the *SHP* MLR and the *HPI* MLR) than $phys_{par}$. This indicates that the hydrological response of the pond is more influenced by precipitation than by maximum pond perimeter. Equations (7), (8), and (9) represent the resulting MLR models.

$$SHP = 0.156 PTOT_{Mar-Jun} + 0.091 Per_{max} + 12.33 \left(R^2 = 0.47, p = 2 \times 10^{-14} \right) \quad (7)$$

$$HPI = 0.0025 PTOT_{Jun-Aug} + 0.0007 Per_{max} - 0.20 \left(R^2 = 0.60, p = 2 \times 10^{-16} \right) \quad (8)$$

$$\log(NRR_{sw}) = -0.0019 PTOT_{Jan-Apr} - 0.0008 Per_{max} + 1.59 \left(R^2 = 0.31, p = 5 \times 10^{-9} \right) \quad (9)$$

The observed *SHP* and *HPI* were reproduced reasonably well by the MLR models (Figure 9), but the model for NRR_{sw} was not able to reproduce satisfactorily observed values.

5 | DISCUSSION

5.1 | Links between pond morphometry and geomorphology

The ponds had contrasting maximum areas, ranging from small basins (HP7) to relatively large basins (HP26). Pond depths were relatively small, reflecting that ponds are generally found in low depressions of the bedrock. As expected and shown also by Brooks and Hayashi (2002), larger ponds held more water. The watershed areas that contributed water to the ponds were highly contrasted but remained

TABLE 1 Results of the multiple linear regression analysis (MLR) of the spring hydroperiod (*SHP*), hydroperiod index (*HPI*), and normalized recession rate of surface water (NRR_{sw}) using precipitation and maximum pond perimeter as explanatory factors (according to Equations 7, 8 and 9).

Hydrological variable	met_{var}		$phys_{par}$	
	$Pr(> t)$	Standardized regression coefficient (β)	$Pr(> t)$	Standardized regression coefficient (β)
<i>SHP</i>	0.0001	0.61	0.0001	0.30
<i>HPI</i>	0.0001	0.73	0.0001	0.30
NRR_{sw}	0.0001	-0.42	0.0001	0.31

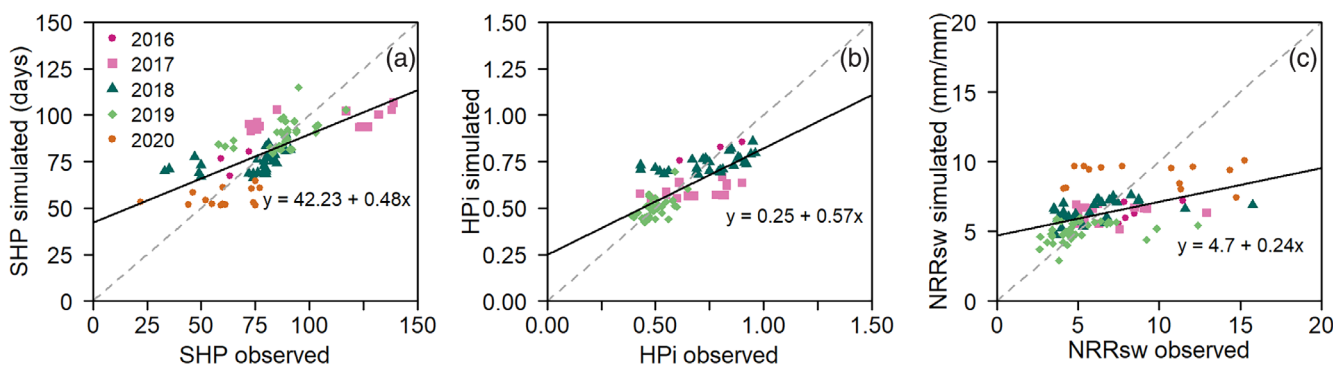


FIGURE 9 Relationship between measured and simulated MLR values for (a) *SHP*, (b) *HPI* and (c) NRR_{sw} . The dashed grey line represents the 1:1 line and the solid black line represents the linear correlation between observed and simulated variables.

relatively small. Interestingly, the watershed areas for some ponds were very small compared to the maximum pond area, that is, WA/A_{max} (e.g., minimum 3.6 at HP27), while others had a much larger ratio (e.g., maximum 170.7 at HP4). Although this ratio was not correlated with altitude, the larger WAs were found in the lower portions of the landscape, which was somewhat expected as ponds located at higher altitudes are also closer to the head of the hydrological watersheds.

The minimum values of the basin profile parameters were similar to those reported in Brooks and Hayashi (2002), but the largest values (e.g., 4.7 at HP27) were higher than those reported by those authors (2.2). The basin profile parameter was not correlated to physical parameters other than those used in Equation (1), indicating that ponds of all sizes and locations had varied basin profiles. The volume–area relationships of the studied ponds were quite diverse, suggesting that information about pond bathymetry is needed to understand pond storage capacity. A simple geometrical representation such as that suggested by Qi et al. (2019) to simulate wetlands storage volumes would not represent the volume–area relationships encountered here.

The high canopy cover over most ponds (median of 82%) was likely influenced by the mostly unaltered conditions in the Kenauk forest. Some ponds might have less canopy cover due to past logging activities around the pond, but this effect is relatively small since a limited number of ponds were affected by logging activities in the last decades (HP6, HP11, HP12, HP13, HP14, HP16, HP19, HP21, HP22, HP24). It is important to note that decreasing canopy cover has been reported for larger ponds in other studies, in areas without any logging activities (Skidds & Golet, 2005; Rhode Island).

The sizes, depths, volumes, and perimeters of the ponds are similar to those of Brooks and Hayashi (2002). Interestingly, sediment thickness, organic matter thickness, watershed size, and canopy cover are seldom reported in the scientific literature. In addition, few studies have reported on ephemeral ponds in the Canadian Shield or other similar igneous fractured bedrocks.

5.2 | Ephemeral pond hydrology

Studies conducted in regions with similar climatic conditions, such as in the northeastern United States, reported very similar annual pond cycles of spring filling to capacity, early summer drying, intermittent rewetting throughout the summer, and refilling in the fall (Brooks, 2004; Straka, 2017). Other studies have shown that ephemeral ponds can remain filled throughout the summer, during particularly wet years (e.g., Batzer et al., 2004). In this current study, even with the humid months of April and May 2017, all the ponds became dry over the summer.

A sufficiently long *SHP* is crucial for amphibians to allow for the metamorphosis of larvae before ponds become dry (Amburgey et al., 2012). In this study, the median *SHPs* were all equal to or higher than 60 days, but lower *SHPs* were observed in 2016, 2018, 2019 and 2020, with values as low as 22 days (2020) and 33 days (2018) monitored at HP9. The minimum duration of *SHP* for amphibian

reproduction to be viable in latitudes such as those of the study area are extremely limited. Studies from the United States report values ranging from 32 to 45 days for American Toads (Skelly & Werner, 1990) to 73–113 days for Wood Frogs (Berven, 1990). COSEWIC (2008) report that the Western Chorus Frog in Canada needs 55–115 days between hatching and complete metamorphosis. Although not all these amphibians can be found in the study area, the shortest *SHPs* observed in this study are likely not sufficient for the successful reproduction of many amphibian species during some years. These results further underline that multi-year and multi-site studies are important for assessing the habitat potential for amphibians.

Interestingly, *SHP* was significantly longer where there were thicker layers of inorganic sediments at the pond bottom (for years 2017 and 2019). This could be due to the relatively low permeability of basal sediments that likely hold water in the pond. The larger ponds also had larger watershed areas and longer *SHPs*. In contrast to other studies (Germandia & Pedrola-Monfort, 2010; Skidds & Golet, 2005), *SHP* was not correlated with maximum pond depth in this study. Results from this study show that pond depth was not related to *SHP* and that pond depth increased the pond recession rate. It is possible that the deeper ponds in the Canadian Shield are more likely to connect with groundwater through sediments and fractured bedrock than they would be in an alluvial plain. Here, the larger WAs appear to contribute to longer *SHPs*, probably because the bigger contributing area provides more groundwater and hypodermic flow to the pond in early summer. Interestingly, no correlations were found between *SHP* and the basin profile coefficient (p), in contrast to results from Brooks and Hayashi (2002). Perhaps some complex pond geometries were not adequately represented by the simple basin profile parameter. Canopy cover was inversely correlated with *SHP* and pond size. Although the water absorption by the trees could be a contributing factor, the smaller ponds may also have simply had shorter *SHPs* because they hold less water (Batzer et al., 2004).

Average *SHPs* did not markedly vary throughout the study period. Nevertheless, *SHPs* in 2020 were significantly shorter than in 2017, 2018 and 2019, and *SHPs* in 2019 were longer than in 2016, 2017 and 2018. These results are directly linked to P and P_{net} , which were particularly low in 2020 and high in 2019. Interestingly, 2019 had the longest average *SHP* but the shortest *HPi*, which is a direct result of 2019 having the wettest spring and the driest July and August of the study period (cf. Table S1). This underlines the importance of continuous monitoring of water levels throughout the period during which there is water in the ponds. Studies have reported that other meteorological variables such as the pattern and timing of rain event intensity, winter conditions for snow accumulation, and soil frost have also been identified as contributing factors to pond hydrology (Brooks, 2009), but these data were not available in this study. Few values for *HPi* exist in the literature, making it difficult to estimate how representative these values are. Except for 2019 (48%), *HPi* values indicated that the ponds were active more than half the time between early April and mid-October.

NRR_{sw} and NRR_{gw} varied markedly between ponds, but NRR_{sw} remained >1 throughout the study period confirming that PET was not the only process responsible for the water level decreases measured at the SW piezometers. Chandler et al. (2017) found similar results in Florida ponds and suggested that groundwater fluxes from the pond to the aquifer might drive water level declines. NRR_{sw} values lower than NRR_{gw} (except for at S2) are somewhat misleading since NRR_{gw} does not include the effect of effective porosity (not measured here) on groundwater level changes. With pond sediment effective porosity of 0.3, median NRR_{gw} varies between 0.93 (S2) and 3.9 (S4), while an effective porosity of 0.1 leads to NRR_{gw} between 0.31 (S2) and 1.3 (S4). These estimations suggest that actual groundwater recession rates are probably smaller than surface water recession rates. The uncertainty in sediment effective porosity does not allow to estimate whether groundwater recession rates are equal or larger than PET. However, it seems probable that PET probably has only a limited effect on groundwater recession rates in this cold and humid climate. Interestingly, groundwater recession rates were very small at S2, probably due to the fine clay sediments in the S2 GWB piezometer. The smaller ponds had higher NRR_{sw} values. They also had denser canopy cover, which could contribute to further increases in NRR_{sw} due to tree transpiration and decreasing groundwater levels. Due to accessibility constraints, pond instrumentation did not include fractured bedrock monitoring wells close to the ponds. Having only groundwater levels in sediment piezometers may have somewhat biased the results, as sediments and fractured bedrock do not react the same way to snowmelt and recharge.

The dominating negative i_v and i_h values for ponds S1 to S5 indicate that groundwater flowed mostly from the pond to the aquifer. For S6, the opposite was observed, with most hydraulic gradients flowing from the aquifer to the pond. However, this is difficult to explain based on the physical parameters of this pond. Positive i_v and i_h occurred sporadically at ponds S1 to S5, especially during the spring period when groundwater levels were highest. The results showed only limited correlations between hydraulic gradients and physical pond parameters.

The correlation analysis showed that total precipitation in spring and early summer (March to June) had the largest effect on SHP . HPI was better explained by summer (June to August) precipitation compared to other periods, which is logical considering summer reactivation largely influences HPI . NRR_{sw} was mostly influenced, albeit only to a limited extent, by winter precipitation (January–April). This might be because winter precipitation is an important driver of snowmelt water input to the hydrosystem, replenishing surface and groundwater reservoirs that reduce recession rates. However, considering that the MLR model for NRR_{sw} was not able to represent satisfactorily observed values, winter precipitation might not be a true causal factor of pond recession rates.

The MLR models reproduced relatively well SHP and HPI , but the R^2 values were not exceptionally high. When comparing simulated and observed values (Figure 9), it is interesting to note that points from different years follow distinct linear relationships. This can be interpreted as an indication that the explanatory variables were not

able to capture the spatial variability between ponds during a given year. This might be related to precipitation gradients on the study area but could not be verified because of a lack of local precipitation data. That the MLR model was not able to reproduce satisfactorily NRR_{sw} could be due to the complexity of the recession process which includes percolation into a variably saturated heterogeneous media. The MLR models are simplistic in nature as they consider only one meteorological variable and one physical parameter. However, the available data from this study, with their inter-site and inter-year variability, did not justify the use of more complex MLR models.

Hydrological models, either simple or more complex, can help us to better understand the hydrological connectivity between ephemeral ponds and their larger-scale hydrological functions (Lee et al., 2020; Montrone et al., 2019). Although models aimed at simulating regional flowrates at river outlets are often not designed to represent processes at the scale of ephemeral ponds, they can be modified to represent specific pond process (e.g., Bizhanimanzar et al., submitted). Although models can be computationally expensive and require detailed pond and watershed data that are often unavailable, they can provide valuable insight into pond watershed flows and the hydrological variables and interactions that cannot be measured in-situ.

5.3 | Insights for pond protection

Although this study used multi-year monitoring data from several ponds, 5 years is a relatively short period of time for this type of assessment. When the MLR models were applied using monthly precipitation data for a 54-year period between 1961 and 2015 for the minimum pond size (25 m), 26% of the years had $SHPs$ below 60 days. For the median pond size (122 m), this percentage fell to 7%, while for the maximum pond size (414 m), all the ponds in all years (100%) had $SHPs$ above 60-days. This indicates that during a dry spring period, the smallest ponds that are often found at higher elevations of watersheds can run dry, but larger ponds that are located at lower elevations can remain active. HPI reached a value of one (i.e., nondrying pond during a specific year) only once in those 54 years for the smallest pond and the median-size pond, but the largest ponds were fully saturated for 17% of those years. Although these are approximate values, they suggest that the largest ponds may not be ephemeral during the wettest summers. Due to the lack of statistical representativity of the MLR model for NRR_{sw} , these values were not estimated for the 1961–2015 period.

The connections observed between groundwater and ponds are indications that groundwater inflow exists in many ponds and that ephemeral pond hydrology is directly linked to the size of the pond watershed area. This implies that it is important to protect the underground areas that contribute to the ponds by protecting groundwater recharge areas, limiting ditches that redirect surface flow, and limiting groundwater pumping. Conversely, hydraulic gradients from the ponds to the sediments are indications that those ponds also help sustain groundwater levels in the aquifer. Protecting ephemeral ponds

could thus be beneficial for groundwater resources (McLaughlin et al., 2014).

The results from this study in conjunction with the predicted increase in spring and fall precipitation (Ouranos, 2023) suggest that *SHP* and *HPI* values will increase while *NRR_{sw}* is expected to decrease. This might mean more years that are suitable for amphibian reproductive success, but it also means more years during which the ponds do not dry, leading to more predators. Aquifer–pond connectivity may also increase, as well a forest-scale connectivity due to higher groundwater levels. Climate-induced shifts have been observed in the past in the Prairie Pothole Region (McKenna et al., 2017), with wetter conditions causing ecosystem shifts. However, the future climate is highly uncertain, and if precipitation increase does not compensate for the increase in evapotranspiration due to higher temperatures, less recharge and dryer conditions could occur (Dubois et al., 2022).

Sustained changes in the hydroperiod could directly affect amphibian reproduction and breeding success or the composition of ephemeral ponds (Brooks, 2009). Protecting ephemeral ponds of different sizes and at different locations in the landscape may help sustain their hydrological and ecosystem functions when hydrological conditions change (Cohen et al., 2016; Evenson et al., 2018). Protecting pond clusters that have a range of *SHPs* could also help cross-reproduction between ponds (Nagel et al., 2021). This can also contribute to ensuring refugia in changing climatic conditions, increasing reproductive success for pond-dependent species (Cartwright et al., 2021). Similar conclusions were reached by Bertassello et al. (2022) who underlined that an increased number of wetlands reduces the variability in amphibian occupancy and contributes the persistence of the Northern Leopard Frog population. Habitat suitability also depends on indirect pressures such as the drainage surrounding the ponds, regional groundwater pumping, changes in land use, changes in water quality, and existing legal protection (Cartwright et al., 2021; Rains et al., 2016).

6 | CONCLUSION

This aim of this study was to identify the geomorphological and meteorological drivers of ephemeral pond hydrology through in-situ characterization and monitoring of 40 ponds in a forest in the Canadian Shield. The ponds were located in the Kenauk forest in the Outaouais region (Quebec, Canada). The ponds were described according to their geomorphological features and monitored for 1–5 years to quantify their spring hydroperiod, hydroperiod index, and recession rates.

This study provides a unique dataset for a large number of ponds over many years in the Canadian Shield forest, an area where ponds are seldom studied. This extensive field-based study confirmed previously reported observations that larger ponds have longer hydroperiods. New data from this study revealed that ponds located at lower altitudes are larger, receive water from a larger area, and have longer hydroperiods than ponds located at higher altitudes. Pond shape did not influence pond hydrology, but mineral sediment thickness increased the hydroperiod. Evapotranspiration was not the only

factor that influenced the pond recession rate and a connection between the ponds and the surrounding saturated geology was demonstrated. Spring and early summer precipitation affected hydroperiods, summer precipitation affected hydroperiod indices, and winter precipitation affected pond recession rates. The multiple regression models were able to simulate hydroperiods and hydroperiod indices relatively well, but pond recession rates were less well reproduced.

This study is one of the few to record the daily fluctuations of hydrological variables in ephemeral ponds over several years. As such, it provides a unique and original database that contributes towards a better understanding of the dynamics of these wetlands, for both meteorological and geomorphological factors. The novel insights from this work will help better understand and protect ephemeral ponds in the forests of cold and humid climates.

ACKNOWLEDGEMENTS

The authors would like to thank NSERC (CRDPJ 506241) and the Sustainable Forest Initiative for their financial support. The authors also thank Kenauk Nature for providing access to the Kenauk forest.

DATA AVAILABILITY STATEMENT

The data that support the findings of this study will be made openly available in the Borealis repository at <https://borealisdata.ca/dataverse/uqam> once the manuscript is accepted for publication.

ORCID

Marie Larocque  <https://orcid.org/0000-0001-9906-3535>

REFERENCES

- Amburgey, S., Funk, W. C., Murphy, M., & Muths, E. (2012). Effects of hydroperiod duration on survival, developmental rate, and size at metamorphosis in boreal chorus frog tadpoles (*Pseudacris maculata*). *Herpetologica*, 68(4), 456–467.
- Batzer, D. P., Palik, B. J., & Buech, R. (2004). Relationships between environmental characteristics and macroinvertebrate communities in seasonal woodland ponds of Minnesota. *Journal of the North American Benthological Society*, 23(1), 50–68.
- Bauder, E. T. (2005). The effects of an unpredictable precipitation regime on vernal pond hydrology. *Freshwater Biology*, 50(12), 2129–2135.
- Bergeron, O. (2016). Guide d'utilisation 2016 – Grilles climatiques quotidiennes du Programme de surveillance du climat du Québec, version 2 (User guide 2016 – Daily climate grids from the Quebec Climate monitoring program, v.2), ministère du Développement durable, de l'Environnement et de la Lutte contre les changements climatiques, Direction du suivi de l'état de l'environnement, Quebec City, Canada.
- Bertassello, L. E., Jawitz, J. W., Bertuzzo, E., Botter, G., Rinaldo, A., Aubeneau, A. F., Hoverman, J. T., & Rao, P. S. C. (2022). Persistence of amphibian metapopulation occupancy in dynamic wetlandscapes. *Landscape Ecology*, 37, 695–711.
- Bertassello, L. E., Rao, P. S. C., Park, J., Jawitz, J. W., & Botter, G. (2018). Stochastic modeling of wetland-groundwater systems. *Advances in Water Resources*, 112, 214–223. <https://doi.org/10.1016/j.advwatres.2017.12.007>
- Berven, K. A. (1990). Factors affecting population fluctuations in larval and adult stages of the wood frog (*Rana sylvatica*). *Ecology*, 71(4), 1599–1608.
- Bizhanimanzar, M., Larocque, M., & Roux, M. (submitted). Development and application of a new soil water assessment tool (SWAT) module to

- simulate ephemeral pond hydrology. *Under Review in Hydrological Processes*.
- Bournival, P., Varin, M., & Fink, J. (2017). Validation d'une méthode semi-automatisée de détection des milieux humides à partir du lidar aéroporté. Centre d'enseignement et de recherche en foresterie de Sainte-Foy inc. (CERFO). Sainte-Foy. Québec (Canada). Report no. 2017-01. 44.
- Brooks, R. T. (2004). Weather-related effects on woodland vernal pond hydrology and hydroperiod. *Wetlands*, 21(1), 104–114.
- Brooks, R. T. (2009). Potential impacts of global climate change on the hydrology and ecology of ephemeral freshwater systems of the forests of the northern United States. *Climate Change*, 95, 469–483.
- Brooks, R. T., & Hayashi, M. (2002). Depth-area-volume and hydroperiod relationships of ephemeral (vernal) forest ponds in southern New England. *Wetlands*, 22(2), 247–255.
- Calhoun, A. J. K., Walls, T. E., Stockwell, S. S., & McCollough, M. (2003). Evaluating vernal ponds as a basis for conservation strategies: A Maine case study. *Wetlands*, 23(1), 70–81.
- Cartwright, J., Morelli, T. L., & Campbell Grant, E. H. (2021). Identifying climate-resistant vernal pools: Hydrologic refugia for amphibian reproduction under droughts and climate change. *Ecohydrology*, 15, e2354. <https://doi.org/10.1002/eco.2354>
- Chandler, H. C., McLaughlin, D. L., Gorman, T. A., McGuire, K. J., Feaga, J. B., & Haas, C. A. (2017). Drying rates of ephemeral wetlands: Implications for breeding amphibians. *Wetlands*, 37, 545–557.
- Cohen, M. J., Creed, I. F., Alexander, L., Basu, N. B., Calhoun, A. J., Craft, C., D'Amico, E., DeKeyser, E., Fowler, L., Golden, H. E., Jawitz, J. W., Kalla, P., Kirkman, K., Lane, C. R., Lang, M., Leibowitz, S. C., Lewis, D. B., Marton, J., McLaughlin, D. L., ... Walls, S. C. (2016). Do geographically isolated wetlands influence landscape functions? *PNAS*, 113(8), 1978–1986. <https://doi.org/10.1073/pnas.1512650113>
- Colburn, E. A. (2004). *Vernal ponds: Natural history and conservation*. McDonald & Woodward Pub. Co.
- COSEWIC (Committee on the Status of Endangered Wildlife in Canada). (2008). COSEWIC assessment and update status report on the Western chorus frog *Pseudacris triseriata* Carolinian population and Great Lakes/St. Lawrence–Canadian shield population in Canada. Committee on the Status of Endangered Wildlife in Canada. Ottawa. 47. www.sararegistry.gc.ca/status/status_e.cfm
- Cui, Q., Ammar, M. E., Irvani, M., Kariyeva, J., & Faramarzi, M. (2021). Regional wetland water storage changes: The influence of future climate on geographically isolated wetlands. *Ecological Indicators*, 120, 106941. <https://doi.org/10.1016/j.ecolind.2020.106941>
- Daigneault, R. A., Roy, M., Lamothe, M., Godbout, P.-M., Milette, S., Leduc, É., North, N., Dubois-Verret, M., Hurtubise, M. A., & Lamarche, O. (2012). *Rapport sur les travaux de cartographie des formations superficielles réalisés dans la portion est du territoire municipalisé de l'Outaouais en 2011–2012* (p. 53). Université du Québec à Montréal. Montréal.
- Dubois, E., Larocque, M., Gagné, S., & Braun, M. (2022). Climate change impacts on groundwater recharge in cold and humid climates: Controlling processes and thresholds. *Climate*, 10, 6. <https://doi.org/10.3390/cli0010006>
- DUC (Ducks Unlimited Canada). (2017). Canards Illimités Canada et le MDDELCC (Ministère du Développement durable, de l'Environnement et de la Lutte contre les changements climatiques). Cartographie détaillée des milieux humides du territoire des basses-terres de l'Outaouais et ses environs-Données géographiques. Québec, Canada, 52.
- Evenson, G. R., Golden, H. E., Lane, C. R., McLaughlin, D. L., & D'Amico, E. (2018). Depressional wetlands affect watershed hydrological, biogeochemical, and ecological functions. *Ecological Applications*, 28(4), 953–966.
- Forget, É., Doyon, F., & Bouffard, D. (2006). *Plan d'aménagement 2006–2015 du territoire Fairmont Kenauk*. Ripon.
- Germandia, A., & Pedrola-Monfort, J. (2010). Simulation model comparing the hydroperiod of temporary ponds with different shapes. *Limnetica*, 20(1), 145–152.
- Hayashi, M., van der Kamp, G., & Rosenberry, D. O. (2016). Hydrology of prairie wetlands: Understanding the integrated surface-water and groundwater processes. *Wetlands*, 36(S2), 237–254. <https://doi.org/10.1007/s13157-016-0797-9>
- Hunter, M. L., Acuña, V., Bauer, D. M., Bell, K. P., Calhoun, A. J. K., Felipe-Lucia, M. R., Fitzsimon, J. A., Gonzalez, E., Kinnison, M., Lindenmayor, D., Lundquist, C. J., Melellin, R. A., Nelson, E. J., & Poschold, P. (2017). Conserving small natural features with large ecological roles: A synthetic overview. *Biological Conservation*, 211, 88–95. <https://doi.org/10.1016/j.biocon.2016.12.020>
- Hynes, A., Clowes, R., & Rivers, T. (2010). Protracted continental collision: Evidence from the Grenville orogen. *Canadian Journal of Earth Sciences*, 47(5), 591–620.
- Klammler, H., Quintero, C. J., Jawitz, J. W., McLaughlin, D. L., & Cohen, M. J. (2020). Local storage dynamics of individual wetlands predict wetlandscape discharge. *Water Resources Research*, 56(11), e2020WR027581.
- Lee, O., Kim, H. S., & Kim, S. (2020). Hydrological simple water balance modeling for increasing geographically isolated doline wetland functions and its application to climate change. *Ecological Engineering*, 149, 105812. <https://doi.org/10.1016/j.ecoleng.2020.105812>
- Malzone, J. M., Sweet, E. G., Bell, A. C., & Minzenberger, G. L. (2019). Geomorphic controls of perched groundwater interaction with natural ridge-top depressional wetlands. *Hydrological Processes*, 34, 1089–1100.
- McKenna, O. P., Mushet, D. M., Rosenberry, D. O., & Lbaugh, J. W. (2017). Evidence for a climate-induced ecohydrological state shift in wetland ecosystems of the southern prairie pothole region. *Climatic Change*, 145, 273–287.
- McLaughlin, D. L., Kaplan, D. A., & Cohen, M. J. (2014). A significant nexus: Geographically isolated wetlands influence landscape hydrology. *Water Resources Research*, 50, 7153–7166. <https://doi.org/10.1002/2013WR015002>
- Montrone, A., Saito, L., Weisberg, P. J., Gosejohan, M., Merriam, K., & Mejia, J. F. (2019). Climate change impacts on vernal pond hydrology and vegetation in northern California. *Journal of Hydrology*, 574, 1003–1013. <https://doi.org/10.1016/j.jhydrol.2019.04.076>
- Nagel, L. D., McNulty, S. A., Schlesinger, M. D., & Gibbs, J. P. (2021). Breeding effort and hydroperiod indicate habitat quality of small, isolated wetlands for amphibians under climate extremes. *Wetlands*, 41, 22. <https://doi.org/10.1007/s13157-021-01404-x>
- Neff, B. P., Rosenberry, D. O., Leibowitz, S. G., Mushet, D. M., Golden, H. E., Rains, M. C., Brooks, J. R., & Lane, C. R. (2020). A hydrologic landscapes perspective on groundwater connectivity of depressional wetlands. *Water*, 12, 50. <https://doi.org/10.3390/w12010050>
- Oudin, L., Hervieu, F., Michel, C., Perrin, C., Andreassian, V., Anctil, F., & Loumagne, C. (2005). Which potential evapotranspiration input for a lumped rainfall–runoff model? Part 2—Towards a simple and efficient potential evapotranspiration model for rainfall–runoff modelling. *Journal of Hydrology*, 303, 290–306.
- Ouranos. (2023). Precipitation–projected changes. <https://www.ouranos.ca/en/precipitations-projected-changes>
- Palik, B., Streblov, D., Egeland, L., & Buech, R. (2007). Landscape variation of seasonal pond plant communities in forests of northern Minnesota, USA. *Wetlands*, 27(1), 12–23.
- Pyke, C. R. (2005). Assessing climate change impacts on vernal pond ecosystems and endemic branchiopods. *Ecosystems*, 8, 95–105. <https://doi.org/10.1007/s10021-004-0086-y>
- Pyzoha, J. E., Callahan, T. J., Sun, G., Trettin, C. C., & Miwa, M. (2008). A conceptual hydrologic model for a forested Carolina bay depressional wetland on the coastal plain of South Carolina, USA. *Hydrological Processes*, 22, 2689–2698.

- Qi, J., Zhang, X., Lee, S., Moglen, G. E., Sadeghi, A. M., & McCarty, G. W. (2019). A coupled surface water storage and subsurface water dynamics model in SWAT for characterizing hydroperiod of geographically isolated wetlands. *Advances in Water Resources*, 131, 103380. <https://doi.org/10.1016/j.advwatres.2019.103380>
- R Core Team. (2020). *R: A language and environment for statistical computing*. R Foundation for Statistical Computing <https://www.R-project.org>
- Rains, M. C., Leibowitz, S. G., Cohen, M. J., Creed, I. F., Golden, H. E., Jawitz, J. W., Kalla, P., Lane, C. R., Lang, M. W., & McLaughlin, D. L. (2016). Geographically isolated wetlands are part of the hydrological landscape. *Hydrological Processes*, 30(1), 153–160.
- Skelly, D. K., & Werner, E. E. (1990). Behavioral and life-historical responses of larval American toads to an odonate predator. *Ecology*, 71(6), 2313–2322.
- Skids, D. E., & Golet, F. C. (2005). Estimating hydroperiod suitability for breeding amphibians in southern Rhode Island seasonal forest ponds. *Wetlands Ecology and Management*, 13(3), 349–366. <https://doi.org/10.1007/s11273-004-7527-4>
- Straka, K. M. (2017). *Characterizing hydrologic fluxes in six Central Maine vernal ponds with a focus on groundwater flow*. University of Maine.
- Tiner, R. W. (2003). Geographically isolated wetlands of the United States. *Wetlands*, 23(3), 494–516.
- Varin, M., Bournival, P., Fink, J., & Chalhaf, B. (2021). Mapping vernal ponds using LiDAR data and multitemporal satellite imagery. *Wetlands*, 41(34). <https://doi.org/10.1007/s13157-021-01422-9>
- Varin, M., Dupuis, M., Bournival, P., & Fink, J. (2015). Acquisition de connaissances essentielles à l'aménagement intégré des ressources sur le territoire Kenauk en Outaouais. Centre d'enseignement et de recherche en foresterie de Sainte-Foy inc. (CERFO). Sainte-Foy. Québec (Canada). 45.
- Werner, E. E., Skelly, D. K., Relyea, R. A., & Yurewicz, K. L. (2007). Amphibian species richness across environmental gradients. *Oikos*, 116(10), 1697–1712. <https://doi.org/10.1111/j.2007.0030-1299.15935.x>

SUPPORTING INFORMATION

Additional supporting information can be found online in the Supporting Information section at the end of this article.

How to cite this article: Roux, M., Larocque, M., Nolet, P., & Bizhanimanzar, M. (2023). Geomorphological and meteorological drivers of ephemeral pond hydrology in the Canadian shield forest. *Hydrological Processes*, 37(10), e15009. <https://doi.org/10.1002/hyp.15009>